

Article

A Numerical Solution for Broadband PLC Splitter with Variable Splitting Ratio Based on Asymmetric Three Waveguide Structures

Hseng-Tsong Wang ¹, Chi-Feng Chen ^{1,2,*} and Sien Chi ³

¹ Institute of Opto-Mechatronics Engineering, Department of Mechanical Engineering, National Central University, Jhongli 32054, Taiwan; aira_wst@hotmail.com

² Department of Mechanical Engineering, National Central University, Jhongli 32054, Taiwan

³ Department of Photonics and Institute of Electro-Optical Engineering, National Chiao Tung University, Hsinchu 30010, Taiwan; schi@mail.nctu.edu.tw

* Correspondence: ccf@ncu.edu.tw; Tel.: +886-3-426-7308

Received: 16 March 2019; Accepted: 7 May 2019; Published: 8 May 2019



Abstract: A numerical solution for the broadband planar-lightwave-circuit (PLC) splitter with a variable splitting ratio based on asymmetric three waveguides weighted by the Blackman weighting function is designed for passive optical network applications with wavelengths between 1.53 and 1.57 μm . The performance of the proposed splitter is verified using the beam propagation method (BPM). It was found that a polynomial function of the splitting ratios accompanying a geometrical shift can be derived from the proposed splitter. The splitting ratio can be changed from 50:50 to 90:10 with this geometrical shift. The excess loss, crosstalk, polarization dependent loss, and splitting ratio variations against wavelength of the proposed splitter with wavelengths between 1.53 and 1.57 μm are better than 0.139 dB, -22.75 dB, 0.006 dB, and 0.335%, respectively. Obviously, the proposed splitter with variable splitting ratio retains the advantages of the symmetric design, such as low excess loss, low crosstalk, polarization insensitivity, broadband, and wavelength insensitivity.

Keywords: adiabatic directional coupler; variable power splitting ratio; blackman weighting function; splitter; waveguide

1. Introduction

For a passive optical network (PON), such as ethernet passive optical network (EPON), gigabit-capable passive optical network (GPON), broadband passive optical network (BPON), and fiber to the x (FTTX), a fiber optic splitter is one of the essential components in the optical fiber link [1]; the 3-dB splitter is one of the most common. However, for network monitoring and flexibility in the PON architecture, a free choice of power splitting ratios is desirable, such as asymmetric Mach–Zehnder interferometers [2]. Moreover, the optic splitters with a broadband characteristic are often required in the wavelength division multiplexing (WDM) applications.

Several power splitting technologies have been developed, such as adiabatic Y branches [3], directional couplers [4], and multimode interference (MMI) couplers [5]. Some special MMI couplers based on special design are proposed to realize the function of arbitrary power splitting ratio, such as surface relief holograms [6], angled structure [7], special butterfly geometrical structure [8], cascaded step-size structure [9], quick response (QR) code-like structure [10], and asymmetric interference structure [11]. Some of those techniques are wavelength sensitive and some are wavelength insensitive. Some of those MMI components are sensitive to wavelength [6–8] while some are wavelength insensitive [9–11]. Arbitrary-ratio power splitters with wavelength insensitivity are appealing for

power splitter applications. In this study, 1×2 MMI power splitters with 1:1, 1:2, 1:3 split ratios by using QR code-like structure are demonstrated [10]. The measured transmission efficiencies of those splitters are near 80% within the range from 1530 to 1560 nm. A 1×2 MMI splitter with arbitrary splitting ratio is numerically and experimentally investigated [11]. The splitting ratio from 100:0 to 50:50 can be obtained by an asymmetric multimode interference (MMI) region, one of which corners is slightly removed. However, the above broadband MMI power splitters still have weak wavelength dependence.

Adiabatic directional couplers (ADCs) with excellent performance for wavelength independence are presented [12–21]. ADCs have other advantages, such as polarization insensitivity [18,19,21] and relaxed fabrication tolerance [18–21]. Two types of ADC were investigated: one with weighted propagation and coupling coefficients [15–21] and the other with constant propagation coefficients and weighted coupling coefficients [12–14]. The coupler with weighted propagation and coupling coefficients results in the structure of coupling-weighted and velocity-tapered waveguides (CVW). CVW couplers have recently made use of an optical switch [15–19] and splitter [20,21]. The gradual change of the CVW structure causes normal mode evolution, which is involved to the changeable propagation and coupling coefficients [15–21]. The properties of switching [15–19] and splitting [20,21] can be obtained as the de-phasing variations and coupling coefficients are appropriately selected. In order to design the slow change of the guide structure, a weighting function should be used [17–21]. A 3-dB CVW splitter weighted by the Blackman weighting function is investigated [21]. It is shown that such 3-dB splitter has some advantages such as low excess loss, low crosstalk, high power uniformity, polarization insensitivity, broadband, and wavelength insensitivity. We aim at designing planar-lightwave-circuit (PLC) splitters with variable splitting-ratio based on the ADCs which are insensitive to wavelength and polarization.

In this paper, we investigate splitters with variable splitting ratios by adjusting the asymmetry of the two side waveguides of the three-waveguide structure for PON applications with wavelengths between 1.53 and 1.57 μm . It was found that when the two side waveguides of the original symmetric three-waveguides structure begin to become asymmetrical, the splitting ratios of the two output ports change accordingly. As the structural asymmetry increases, the difference in splitting ratio between the two output ports also increases. By using the BPM, it is demonstrated that the splitter with variable splitting ratio has excellent performances including excess loss, crosstalk, polarization sensitivity, and wavelength dependence.

2. Theoretical Model

As shown in Figure 1, the variable splitting ratio splitter with coupling-weighted and velocity-tapered waveguides (CVW) structure is composed of three single-mode waveguides. The parameter G_a is the central gap with maximum coupling and G_b is the perturbation. In addition, the width of the narrower port of the waveguide is W_a . The width of the wider port of the waveguide is W_b . Then, H is the height of guide. L_R is the length of two outer guides. The wave propagates in the z -direction. In order to adjust the splitting ratio, a length L_s from the center of the two outer guides is shifted in the z -direction. When the shifting length is set to zero ($L_s = 0$), the device is symmetric in the x -direction relative to guide 0. The width of guide 0 is $(W_a + W_b)/2$. The guide 1 and 2 are velocity-tapered and coupling-weighted. In order to weight the device structure with tapered width and gap, the Blackman function is employed. Two adjacent guides are set tightly that power is able to be coupled by each other. The match point with the maximum coupling coefficient is set in the central position of the outer guide, in which the propagation constant mismatch is zero.

In such an adiabatic coupled-mode system, the standard coupled differential equations describing changes in the mode amplitudes [20] with distance is defined as:

$$\frac{d\bar{a}}{dz} = -i\overline{M}\bar{a} = -i \begin{bmatrix} -\delta_1 & \kappa_1 & 0 \\ \kappa_1 & 0 & \kappa_2 \\ 0 & \kappa_2 & -\delta_2 \end{bmatrix} \cdot \begin{bmatrix} a_1 \\ a_0 \\ a_2 \end{bmatrix}, \tag{1}$$

where $\bar{a} = [a_1 \ a_0 \ a_2]^T$ is a vector containing the amplitudes of the modes in guides 1, 0, and 2. \overline{M} is a 3×3 matrix. δ_1 and δ_2 are the dephasing terms of the structure. κ_1 and κ_2 are the coupling terms of the structure. Those elements of \overline{M} vary with distant z .

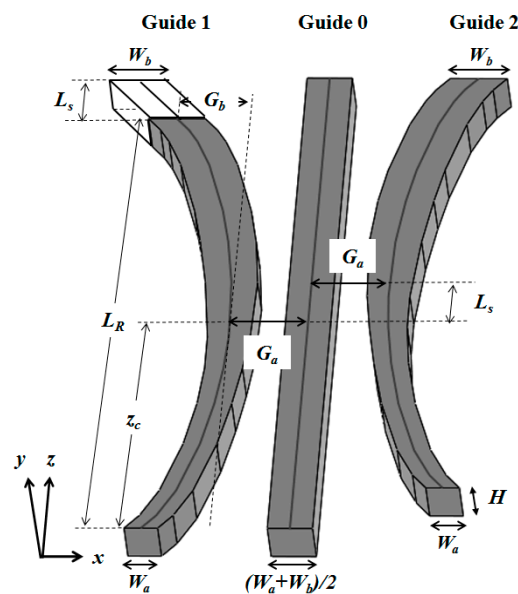


Figure 1. Schematic of the variable splitting ratio splitter with coupling-weighted and velocity-tapered waveguides (CVW) structure.

One particular case occurs as the shifting length is zero ($L_s = 0$), the proposed splitter becomes a symmetric structure which is relative to the center guide, resulting in $\delta_1 = \delta_2 = -\delta$ and $\kappa_1 = \kappa_2 = \kappa$. Full 3-dB power transfer from the center guide to the two outer guides can be achieved [21].

For a small shifting length ($L_s \neq 0$), the coupled-mode amplitudes of (1) results in $\delta_1 \neq \delta_2$ and $\kappa_1 \neq \kappa_2$. As shown in Figure 1, the symmetry of the CVW splitter is broken by shifting guide 2. The power ratio between the two outer guides can be changed by varying the shifting length L_s .

3. BPM Simulation Results and Discussion

In the proposed splitter, the core index is 1.543 and the refractive index of cladding is 1.528 at wavelength $1.55 \mu\text{m}$. In order to keep single-mode [22] operation in C-band, the proposed waveguide height is less than $3.56 \mu\text{m}$ and the width is less than $4.45 \mu\text{m}$. The 3D-BPM [23] is used to evaluate the design concept and the performances of the devices. The fundamental TE mode is launched in the guide 0 for $1.55 \mu\text{m}$ wavelength. Here, an extra section waveguide must be added to the output port of guide 1, as shown in Figure 1, to avoid discontinuities on the output port in 3D-BPM simulation and obtain a meaningful result. The extra guide is considered to keep the cross section and the slope of the guide 1 at $z = L_R$. It can be readily achieved by directly extending the guide 1. Thus, the I/O ports of this extra guide and the output port of guide 1 exhibit the same cross section. The extended waveguide is described as a parallel hexahedron, in which the light energy from guide 1 can be maintained.

The slope of the extended guide can be defined by the derivative of the tapered gap [21] of guide 1 at $z = L_R$. Its length in the z direction is the same as the shifting length L_s .

The seven parameters to be determined are shown in Figure 1. To fulfill the single mode condition, two out of the seven parameters of CVW, the width of the wider port W_b and the height of the waveguide H , can be predetermined. Then, the shifting length L_s is set to zero for 50:50 splitting. Thus, only four parameters are used in the full factorial design method. It was found that a satisfactory result can be obtained to simultaneously satisfy -20 dB crosstalk and equal power splitting in C-band. The results are as follows: $G_a = 6.6$, $G_b = 5.6$, $W_a = 2.6$, $W_b = 4.4$, $H = 3.5 \mu\text{m}$, and $L_R = 3.8$ mm.

The BPM simulation result of power evolution along the z -direction for CVW splitter with the shifting length L_s is shown in Figure 2. One can see that the input power from the center guide can be gradually divided into the two outer guides along the z -direction. In addition, the power output from guide 1 will be greater than that from guide 2.

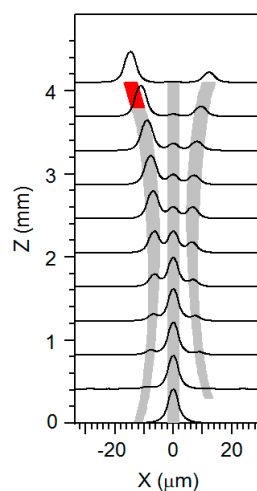


Figure 2. Power evolution for CVW splitter with the shifting length L_s .

The output powers of guide 0, 1, and 2 are represented as P_0 , P_1 , and P_2 , respectively. The crosstalk is the residual power of guide 0. The definition of the excess loss (EL) is the ratio between the total three output powers and the input power. The splitting ratio of guide i ($i = 1$ or 2) is defined as:

$$SR_i = \frac{P_i}{P_1 + P_2} \cdot 100\%, \quad i = 1, 2, \tag{2}$$

Finally, the shifting length L_s is varied to achieve the specified splitting ratio. Eleven shifting lengths spaced equally in the interval 0.05 mm are generated and its corresponding splitting ratios can be obtained by using BPM as shown in Figure 3. The splitting ratio of guide 1 will increase as the shifting length L_s becomes longer. A second-order polynomial curve can be fitted from the eleven-point dataset by using least squares regression. For operating wavelength $1.55 \mu\text{m}$, the splitting ratios of output port guide 1 can be changed by the polynomial function of shifting length L_s , which is expressed as

$$SR_1 = -172.87 (L_s)^2 + 187.93L_s + 49.32, \tag{3}$$

In the regression, the R-squared value is found to be 0.9995 indicating that the curve is rather reliable. According to the polynomial function, the common splitting ratios of 50:50, 60:40, 70:30, 80:20, and 90:10 at operating wavelength $1.55 \mu\text{m}$ could be obtained corresponding to the shifting length of 0, 0.06, 0.124, 0.2, and 0.298 mm, respectively.

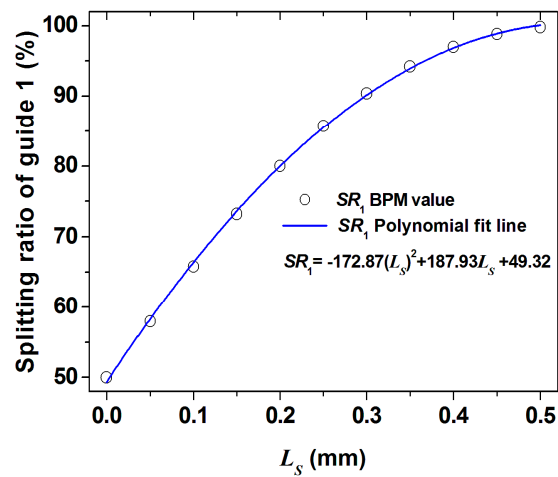


Figure 3. The splitting ratio variations of output port guide 1, as the function of shifting length L_s at wavelength 1.55 μm . The second order polynomial curves of splitting ratio of guide 1 is demonstrated.

In the whole C-band, the average splitting ratios of 50:50, 60:40, 70:30, 80:20, and 90:10 could be achieved by using BPM corresponding to the shifting length of 0, 0.063, 0.128, 0.2, and 0.297 mm, respectively. For C-band, regression analysis is employed to process these five points to derive regression polynomials:

$$SR_1 = -133.82 (L_s)^2 + 175.76 L_s + 49.78, \tag{4}$$

The R-squared value is 0.9996 representing a good fit to the actual data. The polynomial indicates that the average splitting ratio in C-band corresponding to the shifting length L_s can be predicted precisely.

Further analysis on the wavelength dependent of splitting ratio with wavelengths between 1.53 and 1.57 μm at the different shifting length L_s is shown in Figure 4. Five specific splitting ratios of output port guide 1 and guide 2 as the function of wavelength for each specific shifting lengths L_s are presented. When the splitting ratio is adjusted from 50:50 to 90:10, the deviation of the splitting ratio of the splitter with wavelengths between 1.53 and 1.57 μm does not exceed 0.335 from a close examination of the data shown in Figure 4. It indicates that the proposed CVW splitter with variable splitting ratio is wavelength insensitivity.

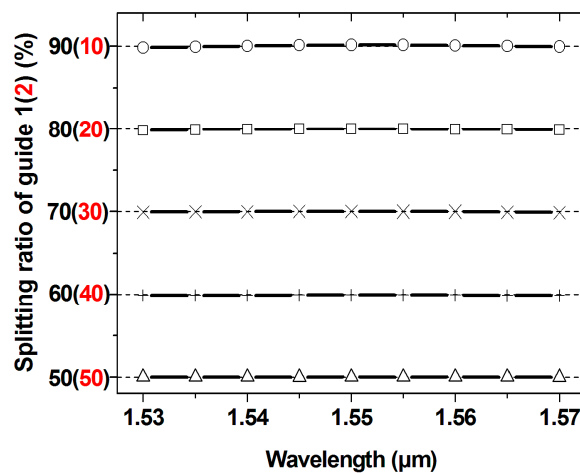


Figure 4. Five specific splitting ratios of output port guide 1 and guide 2 as the function of wavelength for each specific shifting lengths L_s .

In order to further demonstrate the wavelength-insensitive performance of our proposed CVW splitter, we compare the root mean square (RMS) values of the splitting ratio of CVW and MMI [11] splitters. For the 90:10 MMI splitter, the RMS value of the splitting ratio is approximately 0.36 with wavelengths between 1.53 and 1.57 μm . For the proposed 90:10 CVW splitter, the RMS value of the splitting ratio is only 0.11, showing the superior performance of the CVW design.

Figure 5a shows the variations of excess loss with splitting ratios of 50:50, 60:40, 70:30, 80:20, and 90:10 with wavelengths between 1.53 and 1.57 μm . The excess loss of the device for is about 0.111 ~ 0.139 dB. For the MMI splitter [11], the excess loss is less than 0.312 dB while the splitting ratio is adjusted from 50:50 to 90:10 with wavelengths between 1.53 and 1.57 μm . The excess loss of the CVW splitter is 0.173 dB lower than in the MMI splitter. Figure 5b shows that the undesired crosstalk P_0 observed in guide 0 is below -22.75 dB. Those mean that the power transfer of the variable-ratio CVW splitter is stable with low crosstalk and low excess loss with wavelengths between 1.53 and 1.57 μm .

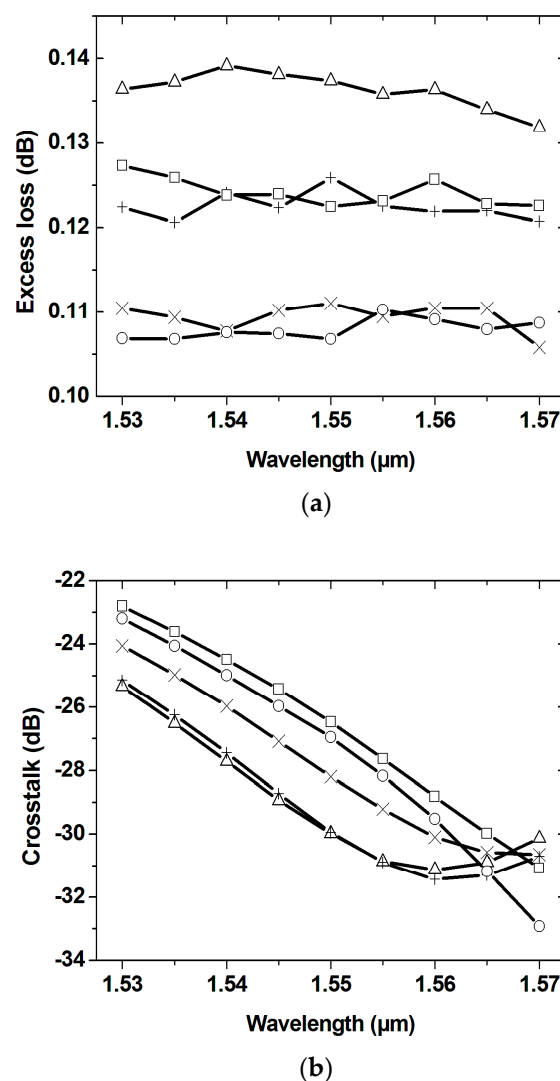


Figure 5. Variations of (a) excess loss and (b) crosstalk with wavelengths between 1530 and 1570 nm. The symbols of splitting ratio: Δ 50:50; + 60:40; \times 70:30; \square 80:20; \circ 90:10.

In order to investigate the polarization effect, the fundamental TM mode is launched in the guide 0. The polarization dependent loss can be written as:

$$PDL = |EL_{TE} - EL_{TM}|, \tag{5}$$

where EL_{TE} is the TE-polarized excess loss and EL_{TM} is the TM-polarized excess loss. Figure 6 shows the variations of the polarization dependent loss in C-band with splitting ratios of 50:50, 60:40, 70:30, 80:20, and 90:10. One can see that all PDL simulation results are less than 0.006 dB. Figure 7 compares the two waveforms of output power guide 1, guide 0, and guide 2 for TE and TM modes with splitting ratio 90:10 at wavelength 1.55 μm . The mean absolute percentage error (MAPE) function is used to evaluate the output waveforms for TE and TM modes. The MAPE value is 1.77%; in other words, the output waveforms for TE and TM modes coincide well. Figures 6 and 7 indicate that the CVW splitter is insensitive to polarization.

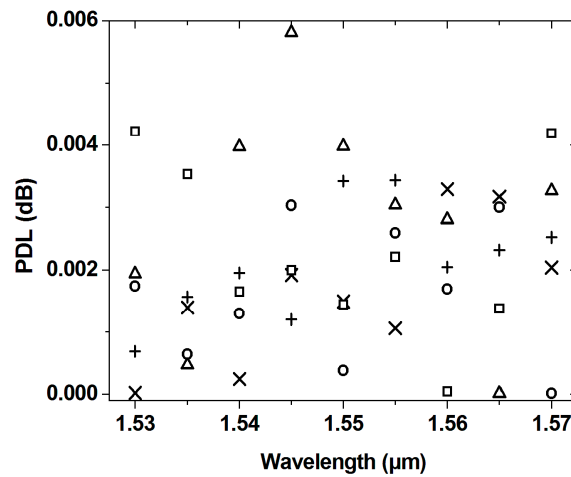


Figure 6. Variations of the polarization dependent loss with wavelengths between 1.53 and 1.57 μm . The symbols of splitting ratio: Δ 50:50; + 60:40; \times 70:30; \square 80:20; \circ 90:10.

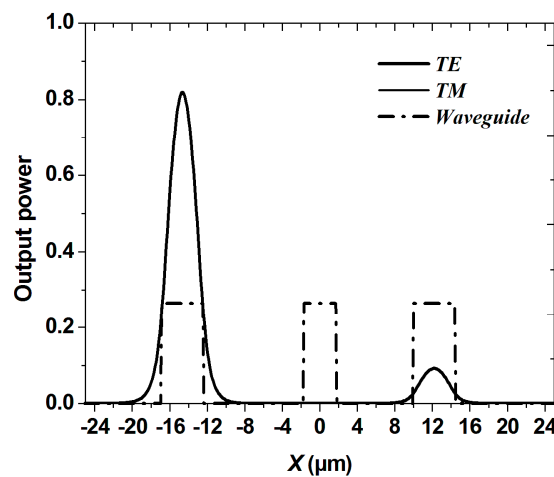


Figure 7. The waveforms of output power guide 1, guide 0 and guide 2 for TE and TM modes with splitting ratio 90:10 at wavelength 1.55 μm . The output waveforms for TE and TM modes coincide well.

Furthermore, splitting ratios for various shifting length L_s and optical performances characteristics are concisely summarized in Table 1. It was found that this proposed splitter with variable splitting ratio can achieve excellent performances such as low crosstalk, low excess loss, wavelength independence, and polarization insensitivity in C-band. Table 2 lists the fabrication tolerance of the design parameters for 90:10 splitting ratio. The allowed splitting ratio deviation and crosstalk are set to $\pm 1\%$ and -20 dB, respectively. For 50:50 splitting, the most sensitive parameter is W_b , the width of the wider port of the waveguide section [21]. However, It was found that the central gap G_a becomes the most sensitive among all parameters for the 90:10 splitting. Figure 8 shows the curve of the splitting ratio against

central gap. It was found that the central gap achieving the 90:10 splitting can be designed at the peak of the curve, which results in higher tolerance.

Table 1. Splitting ratios for various shifting length L_s and optical performances characteristics.

Optical Performances	Splitting Ratio (%)				
	50:50	60:40	70:30	80:20	90:10
Shifting length (mm)	0	0.063	0.128	0.2	0.297
Avg. splitting ratio (%)	50.00:50.00	59.95:40.05	69.99:30.01	79.96:20.04	90.03:9.97
Splitting ratio variation (%) (Max.-min.)	0.030	0.076	0.148	0.184	0.335
Max. excess loss (dB)	0.139	0.126	0.111	0.127	0.111
Max. crosstalk (dB)	-24.97	-24.91	-23.98	-22.75	-23.17
Max. PDL (dB)	0.0058	0.0034	0.0033	0.0042	0.0030
Operate wavelength (μm)	1.53 ~ 1.57				

Table 2. Fabrication tolerance of the design parameters for 90:10 splitting ratio.

Design Parameters	Design Value (μm)	Fabrication Tolerance (μm)	Fabrication Tolerance (%)	Splitting Ratio Penalty (%)	Crosstalk (dB)
G_a	6.6	-0.1 ~ 0	1.52	± 1	<-20
G_b	5.6	-2.4 ~ +1.2	64.29	± 1	<-20
W_a	2.6	-0.1 ~ 0	3.85	± 1	<-20
W_b	4.4	-0.2 ~ 0	4.55	± 1	<-20
H	3.5	-0.3 ~ 0	8.57	± 1	<-20
L_R	3800	-210 ~ +450	17.37	± 1	<-20
L_s	297	-11 ~ +11	7.41	± 1	<-20

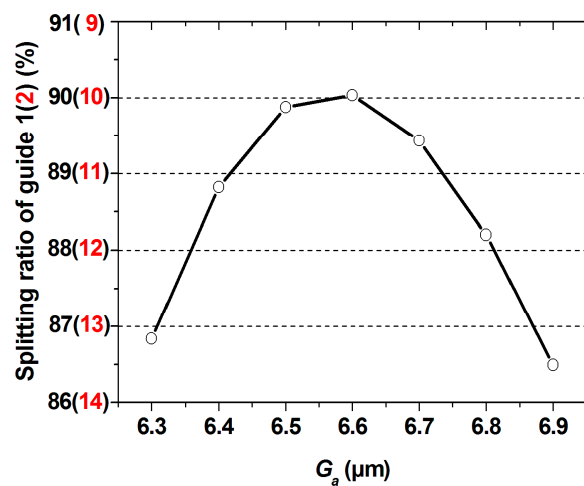


Figure 8. The curve of the splitting ratio against central gap G_a .

4. Conclusions

In this study, a numerical solution for the broadband PLC splitter with variable splitting ratio based on asymmetric three waveguides weighted by the Blackman weighting function was designed for PON applications with wavelengths between 1.53 and 1.57 μm . The performance of the proposed splitter was evaluated by BPM. The two polynomial functions of the splitting ratios accompanying a shifting length were performed. It was found that the splitting ratio could be changed from 50:50 to 90:10 by adjusting the shifting length with wavelengths between 1.53 and 1.57 μm . The excess loss, crosstalk, polarization dependent loss, and splitting ratio variations against wavelength are better than

0.139 dB, −22.75 dB, 0.006 dB, and 0.335%, respectively. Obviously, the variable splitting-ratio splitter with excellent performances is suitable for a variety of PON applications.

Author Contributions: The authors contributed equally to this work, each of them being involved in all research aspects.

Funding: This research received no external funding.

Conflicts of Interest: The authors declare no conflict of interest.

References

- Shumate, P.W. Fiber-to-the-Home: 1977–2007. *J. Lightwave Technol.* **2008**, *26*, 1093–1103. [[CrossRef](#)]
- Moooka, M.; Teruaki, U. Temperature-independent silicon waveguide optical filter. *Opt. Lett.* **2009**, *34*, 599–601.
- Adar, R.; Henry, C.H.; Kazarinov, R.F.; Kistler, R.C.; Weber, G.R. Adiabatic 3-dB couplers, filters, and multiplexers made with silica waveguides on silicon. *J. Lightw. Technol.* **1992**, *10*, 46–50. [[CrossRef](#)]
- Smith, R.B. Analytical solutions for linearly tapered directional couplers. *J. Opt. Soc. Am.* **1976**, *66*, 882–892. [[CrossRef](#)]
- Soldano, L.B.; Pennings, E.C.M. Optical multi-mode interference devices based on self-imaging: principles and applications. *J. Lightw. Technol.* **1995**, *13*, 615–627. [[CrossRef](#)]
- Tseng, S.Y.; Fuentes-Hernandez, C.; Owens, D.; Kippelen, B. Variable splitting ratio 2×2 MMI couplers using multimode waveguide holograms. *Opt. Express* **2007**, *15*, 9015–9021. [[CrossRef](#)]
- Lai, Q.; Bachmann, M.; Hunziker, W.; Besse, P.A.; Melchior, H. Arbitrary ratio power splitters using angled silica on silicon multi-mode interference couplers. *Electron. Lett.* **1996**, *32*, 1576–1577. [[CrossRef](#)]
- Besse, P.A.P.A.; Gini, E.; Bachmann, M.; Melchior, H. New 2×2 and 1×3 multimode interference couplers with free selection of power splitting ratios. *J. Lightw. Technol.* **1996**, *14*, 2286–2293. [[CrossRef](#)]
- Tian, Y.; Qiu, J.; Yu, M.; Huang, Z.; Qiao, Y.; Dong, Z.; Wu, J. Broadband 1×3 couplers with variable splitting ratio using cascaded step-size MMI. *IEEE Photonics J.* **2018**, *10*, 6601008. [[CrossRef](#)]
- Xu, K.; Liu, L.; Wen, X.; Sun, W.; Zhang, N.; Yi, N.; Sun, S.; Xiao, S.; Song, Q. Integrated photonic power divider with arbitrary power ratios. *Opt. Lett.* **2017**, *42*, 855–858. [[CrossRef](#)]
- Deng, Q.; Liu, L.; Li, X.; Zhou, Z. Arbitrary-ratio 1×2 power splitter based on asymmetric multimode interference. *Opt. Lett.* **2014**, *39*, 5590–5593. [[CrossRef](#)]
- Paspalakis, E. Adiabatic three-waveguide directional coupler. *Opt. Commun.* **2006**, *258*, 30–34. [[CrossRef](#)]
- Salandrino, A.; Makris, K.; Christodoulides, D.N.; Lahini, Y.; Silberberg, Y.; Morandotti, R. Analysis of a three-core adiabatic directional coupler. *Opt. Commun.* **2009**, *282*, 4524–4526. [[CrossRef](#)]
- Tseng, S.Y.; Jhang, Y.W. Fast and robust beam coupling in a three waveguide directional coupler. *IEEE Photon. Technol. Lett.* **2013**, *25*, 2478–2481. [[CrossRef](#)]
- Tseng, S.Y.; Wen, R.D.; Chiu, Y.F.; Chen, X. Short and robust directional couplers designed by shortcuts to adiabaticity. *Opt. Express* **2014**, *22*, 18849–18859. [[CrossRef](#)]
- Tseng S., Y. Robust coupled-waveguide devices using shortcuts to adiabaticity. *Opt. Lett.* **2014**, *39*, 6600–6603. [[CrossRef](#)] [[PubMed](#)]
- Syahriar, A.; Schenider, V.M.; Al-Bader, S. The design of mode evolution couplers. *J. Lightw. Technol.* **1998**, *16*, 1907–1914. [[CrossRef](#)]
- Chen, C.F.; Ku, Y.S.; Kung, T.T. Design of short length and C+L-band mismatched optical coupler with waveguide weighted by the Blackman function. *Opt. Commun.* **2009**, *282*, 208–213. [[CrossRef](#)]
- Chen, F. New weighting function designed for low-crosstalk, small length mismatched optical coupler. *Jpn. J. Appl. Phys.* **2010**, *49*, 032501-1–032501-6. [[CrossRef](#)]
- Schneider, V.M.; Hattori, H.T. High-tolerance power splitting in symmetric triple-mode evolution couplers. *IEEE J. Quantum Electron.* **2000**, *36*, 923–930. [[CrossRef](#)]
- Wang, H.T.; Chen, C.F.; Chi, S. A good performance 3-dB splitter based on coupling-weighted and velocity-tapered waveguides. *Opt. Commun.* **2015**, *350*, 97–102. [[CrossRef](#)]

22. Nishihara, H.; Haruna, M.; Suhara, T. *Optical Integrated Circuits*; McGraw-Hill Press: New York, NY, USA, 1989.
23. Huang, W.P.; Xu, C.L. Simulation of three-dimensional optical waveguides by a full-vector beam propagation method. *IEEE J. Quantum Electron.* **1993**, *29*, 2639–2649. [[CrossRef](#)]



© 2019 by the authors. Licensee MDPI, Basel, Switzerland. This article is an open access article distributed under the terms and conditions of the Creative Commons Attribution (CC BY) license (<http://creativecommons.org/licenses/by/4.0/>).